JOURNAL OF CATALYSIS 60, 452–459 (1979)

Influence of the Surface Structure on the Kinetics of Ethane Hydrogenolysis over Ni/SiO_2 Catalysts

G. A. MARTIN

Institut de Recherches sur la Catalyse (C.N.R.S.), 2 Avenue Albert Einstein, 69626 Villeurbanne Cédex, France

Received September 7, 1978

The rate of ethane hydrogenolysis, which was shown previously to be a structure-sensitive reaction, is studied in a large range of pressure and temperature over Ni/SiO_2 catalysts of different morphology. It is observed that the partial reaction order with respect to ethane is unity at low hydrocarbon pressures, and that the partial reaction order with respect to hydrogen and the apparent activation energies vary with hydrogen pressure and temperature. Moreover, orders and apparent activation energies are independent of the nature and of the activity of the catalyst, indicating that the previously reported variations of reaction rate with nickel particle size do not depend on the standard conditions which were chosen. Furthermore, on less active samples, there is no simple relation between the reaction rate, r, and the resulting hydrogen coverage, θ_H (as was the case for a very active sample), from which it is concluded that only a small fraction of the nickel surface is active, (111) planes probably being inactive. On the most active sample, it is supposed that most of the nickel atoms are nearly equivalent from the viewpoint of catalytic activity.

INTRODUCTION

In a recent paper (*1*), we have confirmed that ethane hydrogenolysis over silica-supported nickel catalysts is a structure-sensitive reaction: Increasing nickel particle diameters by thermal sintering in hydrogen results in a large decrease of the areal activity (activity per unit of nickel surface area), in agreement with data reported earlier by Carter *et al.* (*2*). It may be asked, however, whether the observed variations depend upon the temperature and pressure conditions at which this rate was measured. In this paper we report kinetic studies of ethane hydrogenolysis on various nickel samples over a large temperature and pressure range with the aim of answering this question.

Furthermore, we have shown in another paper (*3*) that the rate of reaction, r, over one of the most active catalysts was related to the degree of hydrogen coverage, θ_H, by the following law:

$$r = k_0 e^{-E_0/RT} P_{C_2H_6} \theta_H^{Y} (1 - \theta_H)^{X},$$

where k_0 is nearly equal to the number of ethane molecules colliding with the nickel surface, $E_0 = 14$ kcal/mole, $Y = -1 \pm 2$, and $X = 15 \pm 2$. The rate-limiting step was believed to be ethane adsorption on an ensemble of X adjacent nickel atoms, free from adsorbed hydrogen. Thus it seemed to us of interest to measure the hydrogen coverage of some samples under various conditions of temperature and pressure, in order to establish similar equations. This work was expected to shed some light on the origin

0021-9517/79/150452-08$02.00/0

of the structure sensitivity of ethane hydrogenolysis over nickel.

EXPERIMENTAL

Sample morphology and experimental methods were partially described in previous papers (*1*, *3*, *4*). Most of the Ni/SiO_2 catalysts were obtained by reduction for 15 h in a hydrogen stream of precursors prepared by reacting the support (SiO_2, Aerosil Degussa, 200 m^2/g) with a solution of nickel nitrate hexamine. Reduction temperatures and metallic loadings were varied to obtain different average particle sizes. One of the samples was prepared by reduction (970 K, flowing hydrogen) of nickel antigorite (*5*), which had been pretreated *in vacuo* at 970 K. The exposed faces of nickel particles in this sample were shown to be (111) planes (*6*, *7*).

Magnetic methods were used to study sample morphology (*8*). Degrees of reduction were deduced from saturation magnetization measurements (*4*), and average nickel particle diameters were calculated using the Langevin low- and high-field methods.

Hydrogen and nitrogen adsorption–desorption experiments were performed after evacuation of the reduced catalyst under 10^{-6} Torr at 750 K for 1 h in a classical volumetric apparatus equipped with a Bourdon-type pressure gauge (Texas Instruments).

Kinetics experiments were performed under conditions similar to those previously described (*3*). The diameter of catalyst particles was ca. 0.1 mm. The sample weights were varied from 0.01 to 0.3 g. The total flow was 120 ml/min at room temperature and atmospheric pressure. The ethane partial pressure was 6.3 Torr in most experiments, and conversions were smaller than a few percent. For these conditions, taking into account that the micropore volumes calculated by the B–J–H method (*9*) were large (0.94, 0.91, and 0.42 ml/g, respectively, for samples III, V, and VI in Table 1) and that the BET surface areas were nearly equal to 200 m^2/g for samples I to V and to 90 m^2/g for sample VI, it could be shown that diffusion was not the rate-limiting process (*10*).

RESULTS

Morphology and Hydrogen Adsorption

Most of the results are summarized in Table 1. Degrees of reduction as measured from saturation magnetization were found to be nearly equal to unity for all samples studied. Low-field and high-field methods (*4*) yield surface average diameters, D_s, which are listed in Table 1 (samples I to IV). Sample V was examined in a JEM 100 B electron microscope. Nickel particle diameters span the range 5–15 nm. In addition, a small number of larger particles (50–100 nm) were also observed. On most of the nickel particles small facets could be seen, contrary to the case of samples I, II, and IV obtained by reduction at lower temperatures. Low-field and high-field methods applied to the reversible part of the magnetization-field strength curve lead to diameters, D = 13 and 11 nm, respectively. The corresponding surface diameter is 12 nm. A small remanence (8% of the saturation magnetization) is also observed, indicating that 16% in weight of nickel is made up of large particles. Correcting for these large diameters, and taking for them $D \simeq 75$ nm as suggested by electron microscopy, one obtains the overall surface diameter, D_S = 22 nm, listed in Table 1.

Hydrogen adsorption was studied on samples I, V, and VI and the results were compared to those obtained for sample III (*3*). As previously observed (*3*), a steady equilibrium pressure is rapidly attained after each hydrogen admission (*3*). Adsorption isotherms are best represented by Freundlich relation, $V = kP^a$, as illustrated in Fig. 1 for the case of sample VI. Variations of the exponent a with tem-

TABLE 1

Morphological Characteristics of Catalysts

Sample No.	Ni loadings (%wt)	Reduction temp. (K)	D_S (nm)	D_{H_2} (nm)	V_{H_2} (ml NTP/g Ni)	$P_S \times 10^{-3}$ (Torr)	$r \times 10^{-11a}$
I	4.5	800	2.5	2.5	86	400	6
II	4.5	910	3.6	—	—	—	7.2
III	23	920	6.4	6.3	35	250	8
IV	23	1120	12	—	—	—	1.1
V	23	1200	22	20	11	7	0.65
VI	45[b]	970	[c]	14.5	15	3	1.0

[a] In molecules/s/cm² Ni, measured at 507 K; P_{H_2} = 160 Torr; $P_{C_2H_6}$ = 6.3 Torr.
[b] Nickel antigorite, $Ni_3(OH)_4Si_2O_5$.
[c] Nickel platelet sizes vary from ca. 4 to 15 nm (*6*).

perature are shown in Fig. 2. All isotherms in Fig. 1 converge and meet at the point S, which corresponds to the saturation of the surface (*11*). Similar results were observed for the other samples. The pressures and the volumes of adsorbed hydrogen at saturation, P_S and V_{H_2} are reported in Table 1. If it is assumed (i) that nickel particles are spherical, (ii) that the surface stoichiometry is H/Ni = 1, and (iii) that the cross-sectional area of the surface nickel atom is an average of the values for the (111) and (100) planes, then one can deduce from the volumes at saturation the diameters D_{H_2} listed in Table 1: They are in good agreement with diameters calculated from magnetic measurements.

Isobars at 660 Torr for the different samples are compared in Fig. 3.

Regarding chemisorptive properties, some samples have common features: Compared to samples I and IV, samples V and VI are characterized by larger hydrogen cov-

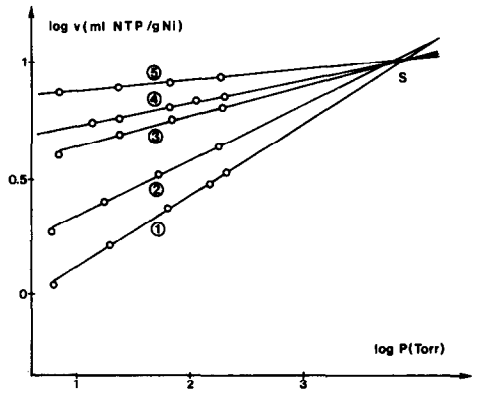

FIG. 1. Log–log isotherms for hydrogen adsorption on sample V at 784, 673, 566, 488, and 273 K (curves 1 to 5).

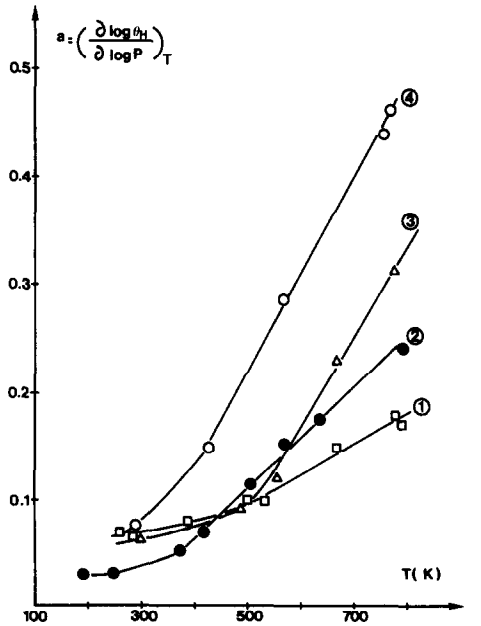

FIG. 2. Exponent a of the Freundlich transform as a function of temperature for samples I, III, V, and VI (curves 1, 2, 3, and 4).

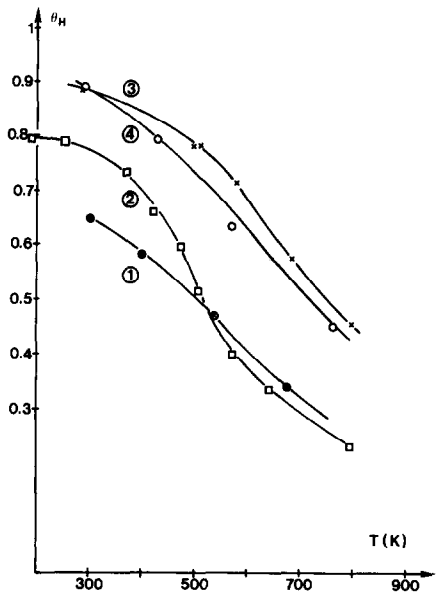

FIG. 3. Isobars for hydrogen adsorption at 660 Torr on samples I, III, V, and VI (curves 1, 2, 3, and 4).

erages (Fig. 3) and lower saturation pressures (see Table 1). This is probably due to a lower repulsive interaction between adsorbed hydrogen atoms on samples V and VI. Moreover, the similar characteristics of samples V and VI suggest that the nature of the exposed faces are similar:

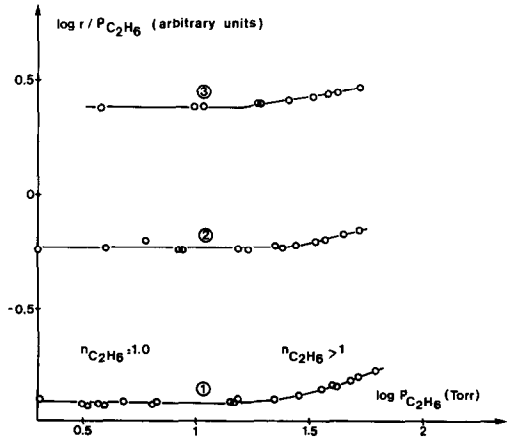

FIG. 4. Reaction partial orders with respect to ethane partial pressure, $n_{C_2H_6}$, on sample V at 566 K and P_{H_2} = 300 Torr (curve 1), at 592 K and P_{H_2} = 300 Torr (curve 2), and at 592 K and P_{H_2} = 660 Torr (curve 3).

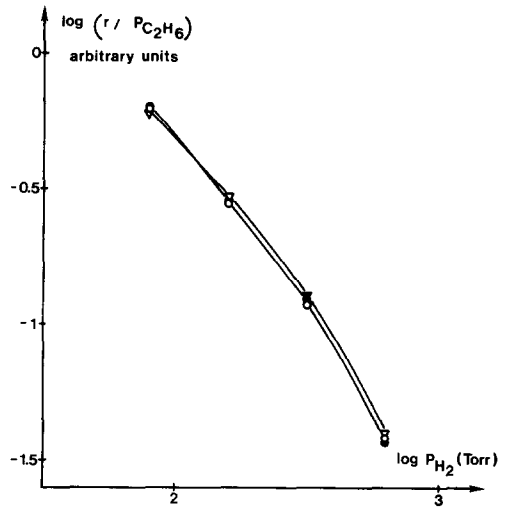

FIG. 5. Log $r/P_{C_2H_6}$ as a function of the log of the hydrogen partial pressure at 566 K, at various ethane partial pressures ($P_{C_2H_6}$ = 25, 10, and 2.5 Torr for triangles, black circles, and open circles, respectively) for samples V.

In other words, the nickel surface of sample V would be made up of (111) planes. This hypothesis is in agreement with the fact that nickel particles in this sample are well faceted.

Kinetic Data

As a first stage, the kinetic study of sample V, the less active catalyst, was performed over a large range of temperature and of pressure. No catalyst-aging phenomena were observed for this sample, as in the case of sample III (*3*). Figure 4 shows that the partial reaction order with respect to ethane pressure is equal to unity below 20 Torr and higher above it, whatever the hydrogen pressure and the temperature. These observations are to be compared with those obtained from the sample III study (*3*) in which two similar reaction orders were also detected. The same explanation can be proposed to account for this unusual behavior at high ethane pressures, namely, that some bimolecular processes occur between gaseous ethane and adsorbed hydrogen species. As for sample IV, we have restricted our study

to the region where the order is equal to unity. In Fig. 5, it is shown that $\log r/P_{C_2H_6}$ against the logarithm of hydrogen pressure is independent of ethane pressure. This means that the partial reaction order with respect to hydrogen pressure (the slope of the curve) is independent of ethane pressure in the range studied. In what follows, the hydrocarbon pressure is maintained constant at 6.3 Torr.

In Fig. 6 reaction rates on sample V are plotted against hydrogen pressure at various temperatures. Corresponding partial reaction orders, n, with respect to hydrogen pressure are negative. Moreover, they vary with temperature and hydrogen pressure, as illustrated in Fig. 7. Variations of apparent activation energy, E_a, with temperature and pressure are similar to those observed for $-n$, and in Fig. 8 a linear relationship is observed between E_a and $-n$, as for sample III.

Let us suppose that the relation between the reaction rate, r, and hydrogen coverage, θ_H, of sample V is similar to that observed for sample III (*3*):

$$r = k(1 - \theta_H)^X.$$

We know (*3*) that this relation is equivalent to

$$n/a = -X\theta_H/(1 - \theta_H),$$

with $a = (\partial \log \theta_H/\partial \log P)T$, the slope of the Freundlich transform, which is independent of the hydrogen pressure P (Fig. 1). Hence, by plotting n/a against $\theta_H/(1 - \theta_H)$, one should obtain a straight line. As a matter of fact, this is observed (Fig. 9), as for sample III (*3*). At variance with this latter, however, is the fact that the parameter X deduced from the slope depends upon temperature, as illustrated in Fig. 10.

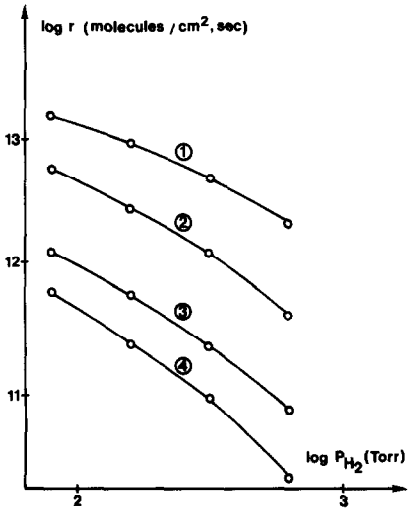

FIG. 6. Reaction partial orders with respect to hydrogen (slopes of $\log r$–$\log P_{H_2}$ curves) at 620, 592, 570, and 549 K (curves 1 to 4) for sample V.

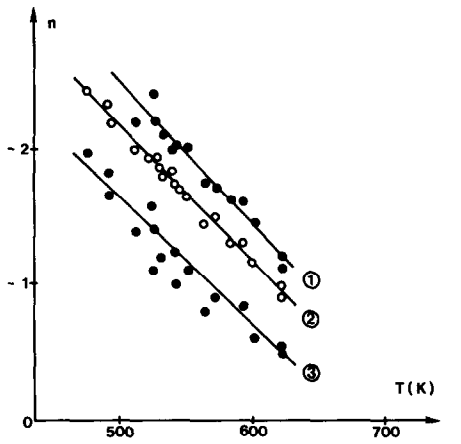

FIG. 7. Reaction partial orders with respect to hydrogen as a function of temperature at various hydrogen partial pressures (630, 300, 63 Torr for curves 1 to 3, respectively) for sample V.

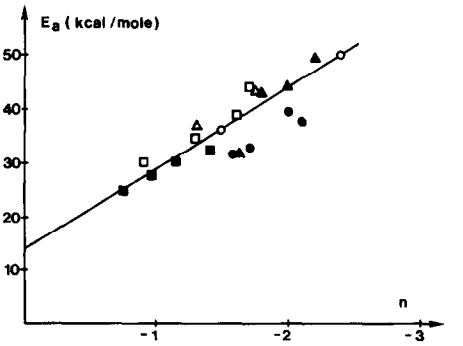

FIG. 8. Apparent activation energies against observed orders with respect to hydrogen partial pressure for sample V: To cover the whole range, sample weights were varied from 0.019 (squares) to 0.293 g (open circles).

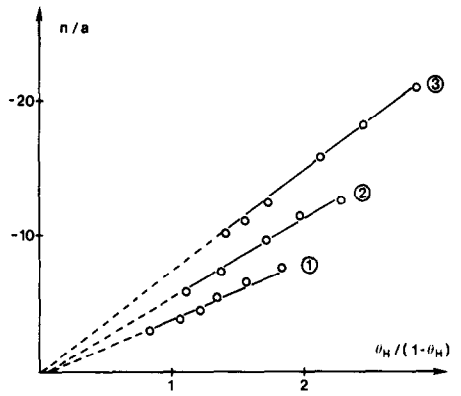

FIG. 9. Variations of the order, n, with respect to hydrogen over a, the exponent of the Freundlich equation, with $\theta_H/(1-\theta_H)$ (θ_H, degree of hydrogen coverage) at 620, 598, and 539 K (curves 1 to 3), for sample V.

Now, how far is the equation $r = k \times (1-\theta_H)^{X(T)}$ capable of accounting for the observed apparent activation energies? If one plots the function $y = (1-\theta_H)^{X(T)}$ against the reciprocal temperature at a given hydrogen pressure, one obtains a straight line, indicating that $E_\theta = (\partial y/\partial 1/T)P$ is independent of temperature. Then, assuming that k may be written as $k = k_0 e^{-E_0/RT}$, we arrive at the conclusion that the apparent activation energy $E_a = E_0 + E_\theta$ is also independent of temperature at constant hydrogen pressure.

This clearly contradicts the observed data, since it has been shown that the apparent activation energy decreases as the temperature T increases (Figs. 7 and 8). Hence, the law $r = k(1-\theta_H)^{X(T)}$, which account for the observed orders, fails to represent the apparent activation energy (in contrast with the corresponding law established for sample III (*3*)), and should be considered as a formal equation which has no physical meaning.

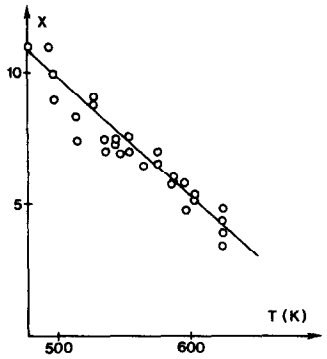

FIG. 10. Exponent X of the equation $r = k(1-\theta_H)^X$ as a function of temperature (sample V).

Very similar kinetic results were obtained for other catalysts in Table 1. The study was restricted to low ethane pressures (6.3 Torr); in those conditions the partial reaction order with respect to ethane is unity. Apparent activation energies, E_a, and partial reaction orders with respect to hydrogen, n, are shown in Figs. 10 and 11, where they can be compared with those observed for samples III and V, and with some data reported in the literature. To a first approximation, they can be considered as nearly identical in given conditions of temperature and pressure.

DISCUSSION

The fact that all samples have the same reaction order and apparent activation energies whatever the temperature and the pressure indicates that the rate equation, r, can be written as $r = k'f(T, P)$: the function $f(T, P)$ is independent of the nature of the sample (of nickel particle size and of the support, as seen in Figs. 10 and 11), and the coefficient k' varies from one sample to another. The first clear conclusion which can be drawn is that the variations of reaction rate with nickel particle size reported in Refs. (*2*) and (*3*) do not depend on the temperature and reactant pressures at which the rate is measured. The observed variations are to be attributed to the coefficient k'.

This suggests that only a part of the surface of the less active samples would be active for ethane hydrogenolysis, and that this part would have the same characteristics as the surface of the most active sample (the same degree of hydrogen cov-

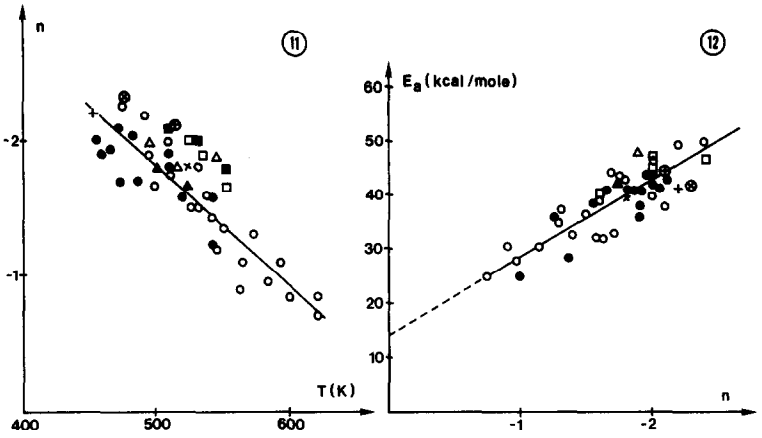

FIG. 11. Reaction partial orders with respect to hydrogen at 300 Torr as a function of temperature: triangles, sample I; black triangles, sample II; black circles, sample III; squares, sample IV; open circles, sample V; black squares, sample VI; +, Ni/SiO_2 (Ref. (*12*)); ×, Ni/Al_2O_3 (Ref. (*12*)); ⊗, Ni/SiO_2 (Ref. (*13*)); ⊕, unsupported nickel catalysts (Ref. (*14*)).

FIG. 12. Apparent activation energies, E_a, against orders with respect to hydrogen partial pressure n for the samples compared in Fig. 11.

erage, the same mechanism, and the same orders and apparent activation energies resulting from the same law $r(\theta_H)$). The ratio, r/r_0 (r_0 being the reaction rate corresponding to the most active sample), would give an idea of the fraction of the active surface area.

Observed degrees of hydrogen coverage for less active samples result from hydrogen adsorption on both active and relatively inactive sites; thus it is understandable why the observed rate has nothing to do with the resultant degree of hydrogen coverage, and why $r = k'(1 - \theta_H)^{X(T)}$ is a purely formal equation in the case of sample V. This emphasizes one of the difficulties which can be encountered in this type of study: When a correlation between the reaction rate, r, and the degree of hydrogen coverage, θ_H, is sought, the sample with the largest fraction of catalytically active surface should be tested. If not, the exponent X of the function $(1 - \theta_H)^X$ could be dramatically underestimated, as illustrated in the case of sample V (Fig. 9).

What is the nature of the less active surface? It is believed that the low activity of samples V and VI can be attributed to the presence of (111) planes which are relatively inactive for the hydrogenolysis reaction (*1*), as already proposed in the case of platinum (*15*). Comparison of the degrees of hydrogen coverages (Fig. 3) allows us to propose a possible explanation for this. It can be seen that samples V and VI (and hence, (111) planes) are more covered by hydrogen than samples I and III. It is striking that the catalysts which have the largest degrees of hydrogen coverage are the least active, as would be suggested by a law of the type $r = k(1 - \theta_H)^X$. It is hazardous to speculate further, however, without accurate kinetic studies over single crystal (111) faces. Moreover, another hypothesis is also plausible: (111) faces might be selectively poisoned by carbonaceous residues.

The last point which deserves some comments is the following: for sample III, a quantitative relationship has been found between θ_H, the resulting hydrogen coverage on all nickel surface atoms of the sample, and r, the rate of ethane hydrogenolysis. This suggests that all nickel atoms susceptible to react with hydrogen

(in fact most of the surface nickel atoms, as shown by the good accordance between D_{H_2} and D_s in Table 1) are nearly equivalent from the standpoint of catalytic activity. This would mean that ethane hydrogenolysis could be considered as a structure-insensitive reaction, on the condition that (111) planes are not considered. This would explain why it has been recently observed by other researchers (*13*) that the activity was independent of nickel particle size in the range 1.5–7.7 nm, in contrast with our data: the reduction temperature used in that work is lower and would not allow faceting and (111) plane formation.

REFERENCES

1. Martin, G. A., and Dalmon, J. A., *C. R. Acad. Sci., Ser. C* **286**, 127 (1978).
2. Carter, J. L., Cusumano, J. A., and Sinfelt, J. H., *J. Phys. Chem.* **70**, 2257 (1966).
3. Martin, G. A., *J. Cat.* **60**, 345–355.
4. Primet, M., Dalmon, J. A., and Martin, G. A., *J. Catal.* **46**, 25 (1977).
5. Martin, G. A., Imelik, B., and Prettre, M., *C. R. Acad. Sci., Ser. C* **264**, 1536 (1967).
6. Dalmai-Imelik, G., Leclercq, C., Massardier, J., and Maubert-Muguet, A., *J. Chim. Phys.* **2**, 176 (1976).
7. Dalmai-Imelik, G., Leclercq, C., and Maubert-Muguet, A., *J. Solid State Chem.* **16**, 1536 (1976).
8. Selwood, P. W., "Chemisorption and Magnetization." Academic Press, New York, 1975.
9. Barrett, E. P., Joyner, L. G., and Halenda, P. H., *J. Amer. Chem. Soc.* **73**, 373 (1951).
10. Satterfield, C. N., and Sherwood, T. K., "The Role of Diffusion in Catalysis." Addison–Wesley, London, 1963.
11. Hayward, D. O., and Trapnell, B. M. W., "Chemisorption," p. 159. Butterworths, London 1964.
12. Sinfelt, J. H., Taylor, W. F., and Yates, D. J. C., *J. Phys. Chem.* **69**, 3857 (1965).
13. Rhyndin, Y. A., Kuznetsov, B. N., and Yermakov, Y. I., *React. Kinet. Catal. Lett.*, **7**, 105 (1977).
14. Sinfelt, J. H., Carter, J. L., and Yates, D. J. C., *J. Catal.* **24**, 283 (1972).
15. Clarke, J. K. A., and Rooney, J. J., *in* "Advances in Catalysis and Related Subjects" (D. D. Eley, H. Pines, and P. B. Weisz, Eds.), Vol. 25, p. 125. Academic Press, New York, 1976.